Life Sciences 226 (2019) 173–184

Contents lists available at ScienceDirect

Life Sciences

journal homepage: www.elsevier.com/locate/lifescie

Postnatal early overfeeding induces cardiovascular dysfunction by oxidative stress in adult male Wistar rats

Marcos Divino Ferreira Junior[a,b], Keilah Valéria Naves Cavalcante[b], Lucas Araújo Ferreira[a], Paulo Ricardo Lopes[b], Carolina Nobre Ribeiro Pontes[c], Amanda de Sá Martins de Bessa[c], Ângela Ribeiro Neves[b], Flávio Andrade Francisco[d], Gustavo Rodrigues Pedrino[b], Carlos Henrique Xavier[e], Paulo Cezar de Freitas Mathias[d], Carlos Henrique de Castro[c], Rodrigo Mello Gomes[a,b,*]

[a] Laboratory of Endocrine Physiology and Metabolism, Federal University of Goiás, Brazil
[b] Neuroscience and Cardiovascular Physiology Research Center, Federal University of Goiás, Brazil
[c] Integrative Laboratory of Cardiovascular and Neurological Pathophysiology, Federal University of Goiás, Brazil
[d] Laboratory of Biology of Cellular Secretion, State University of Maringá, Brazil
[e] Laboratory of Systems Neurobiology, Federal University of Goiás, Brazil

ARTICLE INFO

Keywords:
Postnatal overfeeding
Obesity
Cardiac dysfunction
Vascular dysfunction
Cardiac remodeling

ABSTRACT

Aims: Obesity is associated with innumerous comorbidities, including cardiovascular diseases, that occur by various mechanisms, including hyperactivation of the renin angiotensin system, oxidative stress and cardiovascular overload. Postnatal early overfeeding (PO) leads to metabolic imprinting that induces weight gain throughout life, and in this paper, we aimed to evaluate cardiovascular parameters and cardiac molecular changes due to obesity induced early in life by PO.

Main methods: Male Wistar rats (120-days-old), raised in normal (NL) or small litters (SL), were submitted to cardiac assessment by transthoracic echocardiography and blood pressure evaluation. Thereafter, the hearts and aorta rings from these animals were submitted to *ex-vivo* isolated assays. Still, cardiac morphological and molecular analyses were performed.

Key findings: PO induced ventricular hypertrophy, raised blood pressure, increased fibrosis, and *ex-vivo* cardiac dysfunction in the SL group. Furthermore, SL animals presented impaired vascular relaxation and increased vascular constriction responses. Besides functional alterations, SL animals presented augmented RAB-1b and SOD-1, despite no changes in RAS receptors expression or Akt/eNOS pathway.

Significance: Taken together, our results consolidate the knowledge that the PO during lactation is critical for cardiometabolic programming, leading to oxidative stress and cardiac remodeling in later stages of life.

1. Introduction

Metabolic syndrome (MS) is considered a worldwide pandemic. The prevalence of metabolic syndrome, mainly associated with hypertension, grows amazingly, exceeding the first World Health Organization estimates made in the early 2000s, with predictions up to 35% higher than the WHO estimates for obesity in 2030 [1–3]. The criteria that define the metabolic syndrome consider obesity comorbidities such as visceral fat excess, dyslipidemia and hypertension [4]. In addition, the main factor that contributes to the homeostatic imbalance during MS is the increased body adiposity.

White adipose tissue plays a fundamental role in the obesity-linked alterations. In addition to the energy storage function in the form of triglycerides, it can regulate food behavior, energy balance, vascularization, and others, through hormones and adipokines [5–7]. When adiposity increases, several alterations occur in the morphology of adipose tissue, increasing the secretion of adipokines, which assume a pro-inflammatory profile, attracting immune cells and come into a vicious cycle [8,9]. Studies have shown that this pro-inflammatory state contributes to the development of cardiovascular diseases, and stablishes the relationship between obesity-related effects and probably changes in the Renin Angiotensin System (RAS) [6,8,10–13], and

* Corresponding author at: Department of Physiological Sciences, Biological Sciences Institute II, room 121, Federal University of Goias, Campus II, Esperance Avenue, CEP: 74690-900 Goiania, GO, Brazil.
E-mail address: rodrigomellogomes@hotmail.com (R.M. Gomes).

https://doi.org/10.1016/j.lfs.2019.04.018
Received 7 March 2019; Received in revised form 29 March 2019; Accepted 6 April 2019
Available online 08 April 2019
0024-3205/

impaired insulin sensitivity [14–16].

Cardiac remodeling may be a consequence of activation of RAS, through mitogen-activated Protein Kinases (MAPK), which activate signaling cascades related to cell proliferation and extracellular matrix deposition. Animals whose cardiac local RAS is overactivated developed ventricular hypertrophy, independent of hypertension [17]. This hypertrophy is reflected mainly in cardiac diastolic dysfunction [18]. Moreover, pro-inflammatory profile promote dysfunctional vessels which contribute to increases in blood pressure and cardiac remodeling through augmented post-load, hypertrophy and subsequently higher oxidative stress in the heart [14,19–21].

Furthermore, obesity can be induced in different stages of life, malprogramming the metabolism of diverse organs [22–25]. Epigenetic modifications can occur due to various insults to homeostasis, mainly in critical periods of life, such as fetal period, lactation, and puberty [26,27]. Many studies have focused on the effects of metabolic programming due to disturbances in uterine life [26,28,29] and lactation [30,31]. The animal model of obesity induced by postnatal early overfeeding (PO) through small litter (SL) mimics childhood and juvenile obesity and its effects in adult life, with well-established effects, such as increased adiposity and body weight [24,32]. It was observed that PO animals developed early cardiac epigenetic alterations [32] and increased oxidative stress [23,33]. Additionally, PO impaired cardiac function in aged rats [34].

Although several studies address the cardiovascular alterations due to obesity, few propose to evaluate the differences on cardiac function in presence or absence of neuroendocrine contributions. In this sense, the aim of our study was to evaluate the effects of early obesity metabolic inset, caused by PO, on cardiovascular parameters such as cardiac function and morphology, and vascular contractility in adult postnatal overfed male Wistar rats.

2. Material and methods

The handling of animals and experimental procedures were done according ARRIVE guidelines, National Council of Animal Experiments Control (CONCEA) and the Brazilian Society of Science in Laboratory Animals (SBCAL), and approved by ethics committee of use of animals in research of Federal University of Goiás, under protocol 043/17.

2.1. Animal model

Female and Male Wistar rats aged 70-days-old, from Animal Facility House of Federal University of Goiás, were housed on the Animal Facility house of the Department of Physiological Sciences of Federal University of Goiás, in polypropylene cages (45 × 30 × 15 cm) at controlled temperature (23 ± 2 °C) and light-dark cycle (07:00–19:00). After one week of adaptation, the animals were mated in a ratio of two females (n = 20) to each male (n = 10). Pregnant Wistar rats were housed in individual polypropylene cages with free access to water and food throughout pregnancy and lactation periods.

At delivery, dams were randomly divided in two groups, normal litter (NL – n = 10) and small litter (SL – n = 10). At third postnatal day (PN), NL litters were adjusted to 9 pups and SL litters were adjusted to 3 pups [20]. At PN21 offspring from both litters were weaned (n = 30 male rats per group). After weaning, offspring were housed in collective polypropylene cages (3 animals per cage). For both groups were provided *ad libitum* access to water and standard chow (Nuvilab, Colombo, Paraná, Brazil) from PN21 until PN120. During suckling period, offspring were weighted at PN 3, 7, 14 and 21. After weaning, food intake and body weight were measured weekly.

2.2. Echocardiography

At 120-day-old some offspring, from both groups (n = 5 animals from different litters per group) were anesthetized with ketamine + xylazine (80 mg + 5 mg/kg of BW i.p.; Syntec, São Paulo, Brazil), and submitted to transthoracic echocardiography using an ultrasound system equipped with a 12 MHz transducer (GE HealthCare, Chicago, IL, USA). Left Ventricular (LV) internal diameters (LVID), Interventricular septum thickness (IVS), and LV Posterior Wall thickness were analyzed in diastole and systole (LVPW). End-diastolic and End-systolic volumes (EDV; ESV), Systolic Volume (SV), Ejection Fraction (EF) and Fractional shortening (FS) were calculated through algorithms of the equipment software. Also, through a 7 MHz Doppler transducer, the isovolumetric relaxation time (IVRT) was assessed. All parameters were measured at least three times per animal and was compared between the groups.

2.3. In vivo cardiovascular parameters measurement

At PN119, not fasted animals of each group (n = 6 animals from different litters per group) were anesthetized with Ketamine and Xylazine (100 mg (K) + 10 mg (X) /Kg BW; Syntec, São Paulo, Brazil) and submitted to a surgical procedure to implant a heparinized saline-filled polyethylene catheter (50 U/mL, Hepamax, Blau Pharmaceuticals, Cotia, SP, Brazil) into the abdominal aorta through the right femoral artery for recording blood pressure (BP) and heart rate (HR). After 24 h of catheter implant, at PN120, cardiovascular parameters were recorded in conscious animals. BP signal was obtained by connecting the arterial catheter to a pressure transducer (MLT0699, ADInstruments, Bella Vista, Australia) coupled to an analog amplifier (Bridge Amp, FE221, ADInstruments, Bella Vista, Australia). Data were acquired at a frequency of 2 KHz using an analog/digital converter (PowerLab 4/25, ML845, ADInstruments, Bella Vista, Australia). Systolic Blood Pressure (SBP), Diastolic Blood Pressure (DBP) and Mean Arterial Pressure (MAP), and HR were obtained from the BP signals, with algorithms performed by software (LabChart 7 v7.3.7; ADInstruments, Bella Vista, Australia). The analysis was performed after a period of approximately 30 min, after stabilization of both parameters.

2.4. Isolated heart preparation

Another batch of adult rat offspring (n = 5 animals from different litters per group) were decapitated and the hearts were perfused according to Langendorff technique. After trunk opening, the heart was excised and perfused through the aortic stump with Krebs-Ringer solution (118 mM NaCl, 4.7 mM KCl, 1.25 mM $CaCl_2{\cdot}2H_2O$, 1.20 mM $MgSO_4{\cdot}7H_2O$, 1.20 mM KH_2PO_4, 26.5 mM $NaHCO_3$ and 11.7 mM glucose) at 37 °C with constant oxygenation (5% CO_2 and 95% O_2). A water filled balloon was inserted into the left ventricle and connected to a pressure transducer coupled to a data acquisition system (DataQ Instruments, USA), to acquire intraventricular pressure (IVP). The maximal rate of left ventricular pressure rise (max dP/dt), maximal rate of left ventricular pressure decline (min dP/dt) and heart rate (HR) values were calculated from IVP. The perfusion flow was adjusted to keep the perfusion pressure between 60 and 110 mm Hg. Thereafter, the flow was maintained constant and the coronary vascular resistance (CVR) was calculated by the ratio of the perfusion pressure and coronary flow and normalized by the heart weight. The perfusion pressure was monitored through a transducer connected in parallel to the perfusion system. The sample rate was 1 kHz, and the data passed through a low-pass filter of 50 Hz to minimize interferences from power source. After a basal period (30 to 40 min), the hearts from NL and SL offspring were perfused for an additional 15 min with Krebs-Ringer solution to IVP, Maximum and Minimum dP/dt, Perfusion Pressure (PP), and HR assessment. At the end of experimental protocol, left ventricle was dissected and its mass normalized by tibia length, resulting in the ventricular mass index (VMI).

2.5. Isolated aortic ring preparation and vasocontractility procedures

Thoracic aorta rings (4 mm), from animals used in the isolated heart experiment, were placed in 10 mL organ baths at 37 °C containing gassed (95% O_2 and 5% CO_2) Krebs-Henseleit solution (118 mM NaCl, 4.6 mM KCl, 3.3 mM $CaCl_2{\cdot}2H_2O$, 2.4 mM $MgSO_4{\cdot}7H_2O$, 0.9 mM KH_2PO_4, 24.9 mM $NaHCO_3$, 11.1 mM Glucose). Two of the rings had the endothelium removed (E−) by gently rubbing the intimal surface with the support hook itself, and two had the endothelium preserved (E+). Isometric force was evaluated using a force transducer connected to a data acquisition system (DataQ Instruments, USA). After preparation, the rings were initially stretched until the resting tension reached 1.5 g and allowed to equilibrate for 1 h, and readjusted to 1.5 g if necessary. Endothelium-dependent relaxation was performed with Acetylcholine (ACh; 10 μM) after pre-contraction with Phenylephrine (Phe; 0.1 μM) to evaluate the endothelium viability. The integrity of the endothelium was observed in the rings that achieved contraction > 60% of basal value, and relaxation above 80% of maximum contraction. After viability test, a 30-minute period for the stabilization of the preparation and exchange of nutrient solution, a pre-contraction of aorta rings was performed (Phe; 0.1 μM). Then, the E+ preparations were submitted to the concentration curve of ACh (−9; −8.5; −8; −7.5; −7; −6.5; −6; −5.5 and −5 Log mol/L), and the E− were submitted to the concentration curve of Sodium Nitroprusside (−11; −10.5; −10; −9.5; −9; −8.5; −8; −7.5; −7; −6.5; −6.5.5 and −5 Log mol/L). Relaxant responses were analyzed individually. Following the evaluation of relaxation, after a new period of 30 min for stabilization of the preparation and exchange of the nutrient solution, E− contractile response was assessed thought a concentration curve of Phe (−9; −8.5; −8; 7.5; −7; −6.5; −6; −5.5; −5 Log mol/L).

2.6. Euthanasia and samples collection

At PN120, at the end of the experimental period, after a 12-hour fast, another batch of animals (n = 10 animals from different litters to each group) were anesthetized with Thiopental Sodium plus Lidocaine (40 mg/kg of BW, i.p.; Thiopentax, Cristália, Brazil; 1 mg/kg of BW, i.p.; Cristália, Blau Pharmaceuticals, Cotia, SP, Brazil) and euthanized by exsanguination for blood, heart, tibia and retroperitoneal, periepididymal and mesenteric white adipose tissue (WAT) samples collection. Heart and WAT samples were weighed, and tibia were measured. Blood samples were centrifuged for plasma collection (1500*g*, for 15 min), and plasma stored at −20 °C for further analysis.

2.7. Biochemical assays

Plasma levels of Triglycerides, Total Cholesterol and HDL Cholesterol were measured by enzymatic-colorimetric methods (Gold Analisa, Belo Horizonte, Minas Gerais, Brazil) with commercial kits, following the manufacturer's information. Results were expressed as mg/dL. LDL fraction of cholesterol were estimated according Friedewald et al. [35] (LDL = CT − [HDL + {TGC / 5}]), and results were expressed in mg/dL.

2.8. Histological analysis

Heart samples were fixed in formalin solution (10%) and included in histological paraffin (Histopar, Easypath, São Paulo, Brazil). Subsequently, samples were sectioned on a microtome (RM2245, Leica Microsystems, Wetzlar, Germany) in non-serial cuts of 6 μm thickness and stained with Picrosirius Red and counter-stained with Hematoxylin. Photomicrographs were made in a light microscope coupled to a digital camera (DM500 plus ICC50 HD, Leica Microsystems, Wetzlar, Germany), amplified 1000× for the measurement of left ventricle cardiomyocytes (100 cardiomyocytes/group), 100× for measurement of perivascular fibrosis (25 images/group), and 100× for interstitial fibrosis (50 images/group). Photomicrographs of transverse sections of left ventricular cardiomyocytes were analyzed. The distance between the upper and lower parts of the plasmatic membrane was measured at the height of the nucleus of each measured cardiomyocyte. The mean and standard error of cardiomyocyte diameter were calculated for each animal, and the results compared between the groups. Photomicrographs containing collagen marking in fields where cross-sectional arterioles exist were analyzed. The perivascular fibrosis index (PFI) was determined by the division of total fibrosis area and the area of vessel lumen. Interstitial Fibrosis was analyzed by stereology, using a mesh made up of 300 test points. Interstitial fibrosis percentage was estimated by the ratio between the number of points that hit the red marked collagen and total test points. The mean and standard error of the mean of the PFI and Interstitial Fibrosis percentage for each animal were calculated, and the results compared between the groups. Cardiomyocytes diameter and PFI analyses were performed using ICY software (Institut Pasteur, Paris, France). Interstitial Fibrosis was performed using Image Pro Plus v6 (Media Cybernetics, MD, USA).

2.9. Western blot

Left Ventricle Samples (n = 4 animals from different litters to each group) were homogenized in lysis buffer (PBS [137 mM NaCl, 2.4 mM KCl, 10 mM Na_2HPO_4, 1.8 mM KH_2PO_4, pH 7.4], 8.8 mM IGEPAL CA-630, 12 mM Sodium Deoxycholate, 3.47 mM SDS, 2 mM Na_3VO_4, 1 mM PMSF, 2.34 μM Leupeptin, 0.154 μM Aprotinin, 1.45 μM Pepstatin) in a glass homogenizer at 4 °C. Tissue extracts were centrifuged at 10,000 rpm at 4 °C for 20 min to precipitate insoluble material and collection of the supernatant. After centrifugation, supernatant total protein content was quantified by the Bicinchoninic Acid method (Sigma-Aldrich, Missouri, EUA), according manufacturer instructions. The samples were denatured in Laemmli buffer (50 mM Tris-HCl, pH 6.8, 10% Glycerol, 2% SDS, 1% 2-mercaptoethanol, 0.001% bromophenol blue) and heated at 95 °C for 3 min. Aliquots of 40 μg of proteins from each sample were subjected to separation by SDS-PAGE. The efficiency of the separation was accompanied by a positive control with pre-determined staining (Precision Plus Protein Standards, Bio-Rad, Hercules, CA, USA). Separated proteins on the gel were transferred to nitrocellulose membranes (Amersham Protran, GE Healthcare, Little Chalfont, BUX, UK) in a wet transfer system, soaked in transference buffer (20% Metanol, 0.1% SDS, 0.25 mM Tris, 0.19 mM Glycine). The membranes were incubated with a blocking solution (5% skim powdered milk, 10 mM Tris, 150 mM NaCl, 0.02% Tween 20) under mild agitation for 90 min at room temperature, and subsequently incubated with primary antibodies listed in Table 1. Then, the membranes were gently washed (3 × 5 min; 10 mM Tris, 150 mM NaCl, 0.02% Tween 20) and incubated with the manufacturer specific HRP-conjugated secondary antibody (Table 1) for 90 min, and covered with chemiluminescence detection solution (Amersham ECL, GE Healthcare, Little Chalfont, BUX, UK). The chemiluminescence was detected by an image documentation system (ImageQuant LAS 4000 series, GE Healthcare, Chicago, IL, USA), and images were captured. The intensity of the bands was quantified by relative optical density using FIJI software (ImageJ, NIH, Cambridge, MA, USA). GAPDH (Glyceraldehyde-3-Phosphate Dehydrogenase) was used as load control.

2.10. Statistical analysis

Data are expressed as Mean ± Standard Error of Mean (M ± SEM). To compare differences between groups, unpaired Student's *t*-test was used, and level of significance was set at $p < 0.05$. To compare the differences in body weight, food intake and concentrations of drugs on vasocontractility responses in aortic rings, Two-Way ANOVA was used, followed by the Sidak *post-hoc* test, with level of significance was set at $p < 0.05$. Prism 6 version 6.01 software (GraphPad, San Diego, CA, USA) was used for data analysis and build graphics.

Table 1
List of antibodies used for western immunoblotting.

Antibody	Manufacturer and catalog #	Source	Dilution
Anti-AT1R	Santa Cruz, CA, USA (SC-515884)	Mouse monoclonal	1:1000
Anti-AT2R	Booster, CA, USA (M00432)	Rabbit monoclonal	1:1000
Anti-MAS1	Santa Cruz, CA, USA (SC-390453)	Mouse monoclonal	1:1000
Anti-pAKT (Ser473)	Cell Signaling, MA, USA (9271S)	Rabbit polyclonal	1:1000
Anti-AKT	Cell Signaling, MA, USA (9272S)	Rabbit polyclonal	1:1000
Anti-pENOS (Thr495)	Cell Signaling, MA, USA (9574S)	Rabbit polyclonal	1:1000
Anti-ENOS	Cell Signaling, MA, USA (9752S)	Rabbit polyclonal	1:1000
Anti-CAT	LifeSpan, WA, USA (LS-C21346)	Rabbit polyclonal	1:1000
Anti-SOD-1	Santa Cruz, CA, USA (SC-11407)	Rabbit polyclonal	1:200
Anti-RAB1-B	Santa Cruz, CA, USA (SC-599)	Rabbit polyclonal	1:1000
Anti-GAPDH	Santa Cruz, CA, USA (SC-25778)	Rabbit polyclonal	1:1000
Anti-Rabbit IgG-HRP	Santa Cruz, CA, USA (SC-2004)	Goat	1:2000
Anti-Mouse IgG-HRP	Santa Cruz, CA, USA (SC-2005)	Goat	1:2000

3. Results

3.1. Effects of postnatal early overfeeding on biometrical and biochemical parameters

SL offspring presented higher body weight from seventh PN day until PN120 compared to NL offspring ($p < 0.05$; Fig. 1A and B). In addition, food intake of SL animals was higher throughout the experimental period after weaning (Fig. 1C). Furthermore, the area under curve of food intake was higher in SL offspring than NL offspring (NL 313.2 ± 4.1 *vs* SL 343.4 ± 6.3 A.U.; $p = 0.0014$; Fig. 1D). Nonetheless, the SL group had greater adiposity (NL 0.0311 ± 0.002 *vs* SL 0.0456 ± 0.004 g/BW; $p < 0.01$; Fig. 1E), including mesenteric (NL 0.0072 ± 0.001 *vs* SL 0.0103 ± 0.001 g/BW; $p = 0.0142$; Fig. 1F) WAT mass. The hearts mass, normalized to tibia length, of the SL group were approximately 13% heavier than those of their controls (NL 0.316 ± 0.009 *vs* SL 0.356 ± 0.007 g/BW; $p = 0.0049$; Fig. 1G). In addition, SL animals presented high tibia lengths (NL 3.968 ± 0.0190 *vs* SL 4.060 ± 0.0356 cm; $p = 0.0288$; Fig. 1H).

Despite, no differences in total cholesterol (NL 52.4 ± 3.8 *vs* SL 63.7 ± 5.6 mg/dL; $p = 0.1245$; Fig. 1J), and estimated LDLc (NL 23.2 ± 2.9 *vs* SL 30.5 ± 5.7 mg/dL; $p = 0.2791$; Fig. 1L), SL group had altered lipid profile, with increased plasma triglycerides (NL 39.3 ± 2.4 *vs* SL 46.5 ± 1.3 mg/dL; $p = 0.0189$; Fig. 1I) and lower HDLc levels (NL 26.1 ± 1.1 *vs* SL 19.4 ± 1.1 mg/dL, $p = 0.0019$; Fig. 1K).

3.2. Effects of postnatal early overfeeding on cardiac function, morphology and angiotensin receptors expression

Postnatal Overfeeding increased IVS thickness during the diastole (NL 0.13 ± 0.008 *vs* SL 0.16 ± 0.005 cm; $p = 0.0326$; Fig. 2A) and during the systole (NL 0.16 ± 0.013 *vs* SL 0.25 ± 0.011 cm; $p = 0.0018$; Fig. 2A) in SL offspring in relation to NL animals. Similarly, LVPW was 21% higher in SL offspring during the diastole (NL 0.14 ± 0.004 *vs* SL 0.17 ± 0.009 cm; $p = 0.0248$; Fig. 2B) and 27% higher during the systole (NL 0.22 ± 0.01 *vs* SL 0.28 ± 0.02 cm; $p = 0.0447$; Fig. 2B) as compared to NL offspring. However, SL offspring did not present differences in LVID, SV, EF, FS, TRIV and HR (Fig. 2C–I).

Table 2 shows the effect of PO on blood pressure parameters unanesthetized rats. SL animals presented higher values of mean arterial pressure characterized by an increase in both systolic and diastolic components, no differences were observed in heart rate.

As observed in Fig. 3, PO decreased End Ventricular Systolic Pressure (EVSP; NL 130.3 ± 4.93 *vs* SL 103.8 ± 4.48 mm Hg; $p = 0.0061$; Fig. 3A), max dP/dt (NL 3622 ± 135.6 *vs.* SL 2848 ± 159.1; $p = 0.0074$; Fig. 3B) min dP/dt (2443 ± 63.2 *vs* SL 1909 ± 121.3; $p = 0.0042$; Fig. 3C), and CVR (NL 2.893 ± 0.1594 *vs.* SL 2.205 ± 0.2076 mm Hg/heart weight; $p = 0.0316$; Fig. 3E). In addition, SL offspring showed higher associated to a higher VMI (NL 0.18 ± 0.03 *vs* SL 0.29 ± 0.01 g/cm; $p = 0.0234$; Fig. 3F), when compared to NL offspring. No changes in HR was observed (NL 264.7 ± 7.7 *vs* SL 279.4 ± 8.3 bpm; $p = 0.2548$; Fig. 3D).

Furthermore, SL offspring showed increase in cardiomyocyte diameter (NL 12.9 ± 0.3 *vs* SL 14.0 ± 0.2 μm; $p = 0.0097$; Fig. 4A) compared with NL group. In addition, quantitative analysis shows significant increase of the perivascular fibrosis index (NL 4.3 ± 0.4 *vs* SL 5.9 ± 0.4; $p = 0.0291$; Fig. 4D) and interstitial fibrosis (NL 7.77 ± 0.445 *vs* SL 9.79 ± 0.454%; $p = 0.013$; Fig. 4G).

To evaluate angiotensin signaling in the heart of adult offspring, western blot analysis was performed. As shown in Fig. 6, postnatal overfeeding induced no changes in AT1R (NL 100.0 ± 2.9 *vs* SL 99.6 ± 6.5% of control, $p = 0.9631$; Fig. 4J), AT2R (NL 100.0 ± 19.1 *vs* SL 113.4 ± 20.7% of control, $p = 0.6517$; Fig. 4K) or MASR (NL 100.0 ± 8.9 *vs* SL 103.7 ± 11.9% of control, $p = 0.8104$; Fig. 4L).

3.3. Effects of postnatal early overfeeding on Akt, eNOS, CAT, SOD-1 and RAB1-b expression in the heart

Fig. 5 illustrates the effect of PO on Akt, eNOS, CAT, SOD-1 and RAB1-b expression in the heart. Cardiac p-Akt/Akt ratio (NL 100.0 ± 1.6 *vs* SL 105.4 ± 2.5% of control, $p = 0.1259$; Fig. 5A) and total Akt (NL 100.0 ± 7.6 *vs* SL 85.7 ± 3.9% of control, $p = 0.1482$; Fig. 5B) expression were similar in both groups. Likewise, PO did not change peNOS/eNOS ratio (NL 100.0 ± 5.0 *vs* SL 102.5 ± 7.9% of control, $p = 0.8008$; Fig. 5C) and total eNOS content (NL 100.0 ± 5.2 *vs* SL 103.6 ± 12.3% of control, $p = 0.7948$; Fig. 5D). CAT content was not different (NL 100.0 ± 4.0 *vs* SL 98.4 ± 6.9% of control, $p = 0.8446$; Fig. 5F). However, PO increases SOD-1 (NL 100.0 ± 2.4 *vs* 124.2 ± 10.5% of control; $p = 0.0476$; Fig. 5E) and RAB-1b (NL 100.0 ± 1.4 *vs* SL 115.9 ± 5.9% of control, $p = 0.0405$; Fig. 5G) expression in the heart from SL animals.

3.4. Effects of postnatal early overfeeding on aortic vascular reactivity

The endothelium-dependent vascular relaxation response to Ach was significantly reduced in aortic rings from SL rats at concentrations between −6.5 and − 5.5 Log mol/L compared with NL rats (Fig. 6A). However, non-endothelium-dependent vascular relaxation response to sodium nitroprusside was the same in both groups (Fig. 6B). Interestingly, contractile response to phenylephrine was increased in aortic rings from SL animals (Fig. 6C).

4. Discussion

In this study, we demonstrated that PO lead to changes in functional, morphologic and molecular parameters in the hearts of adult

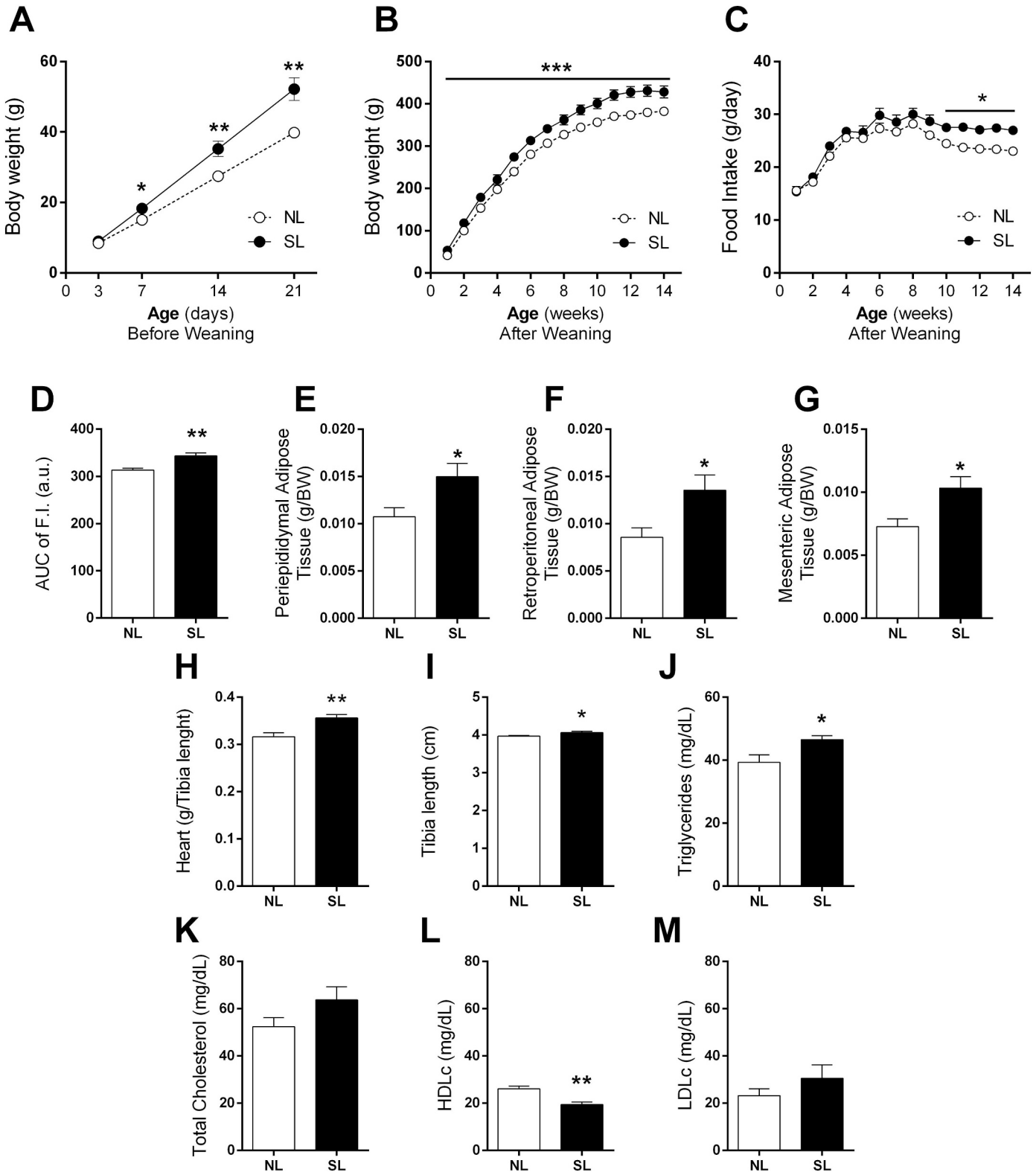

Fig. 1. Effects of postnatal early overfeeding on biometrical and biochemical parameters. Body weight before weaning (A), body weight after weaning until PN120 (B), curve of food intake (C), area under curve (AUC) of food intake (D). Data are presented as the mean ± SEM. Unpaired Student's *t*-test (n = 8–10 litters per group). *p < 0.05, **p < 0.01 and ***p < 0.001 *vs* NL. Periepididymal (E), retroperitoneal (F) and mesenteric (G) adipose tissue, heart weight (H), tibia length (I), triglycerides (J), total cholesterol (K), HDLc (L) and LDLc (M). Data are presented as the mean ± SEM. Unpaired Student's *t*-test (n = 8–10 animals from different litters per group). *p < 0.05 and **p < 0.01 *vs* NL.

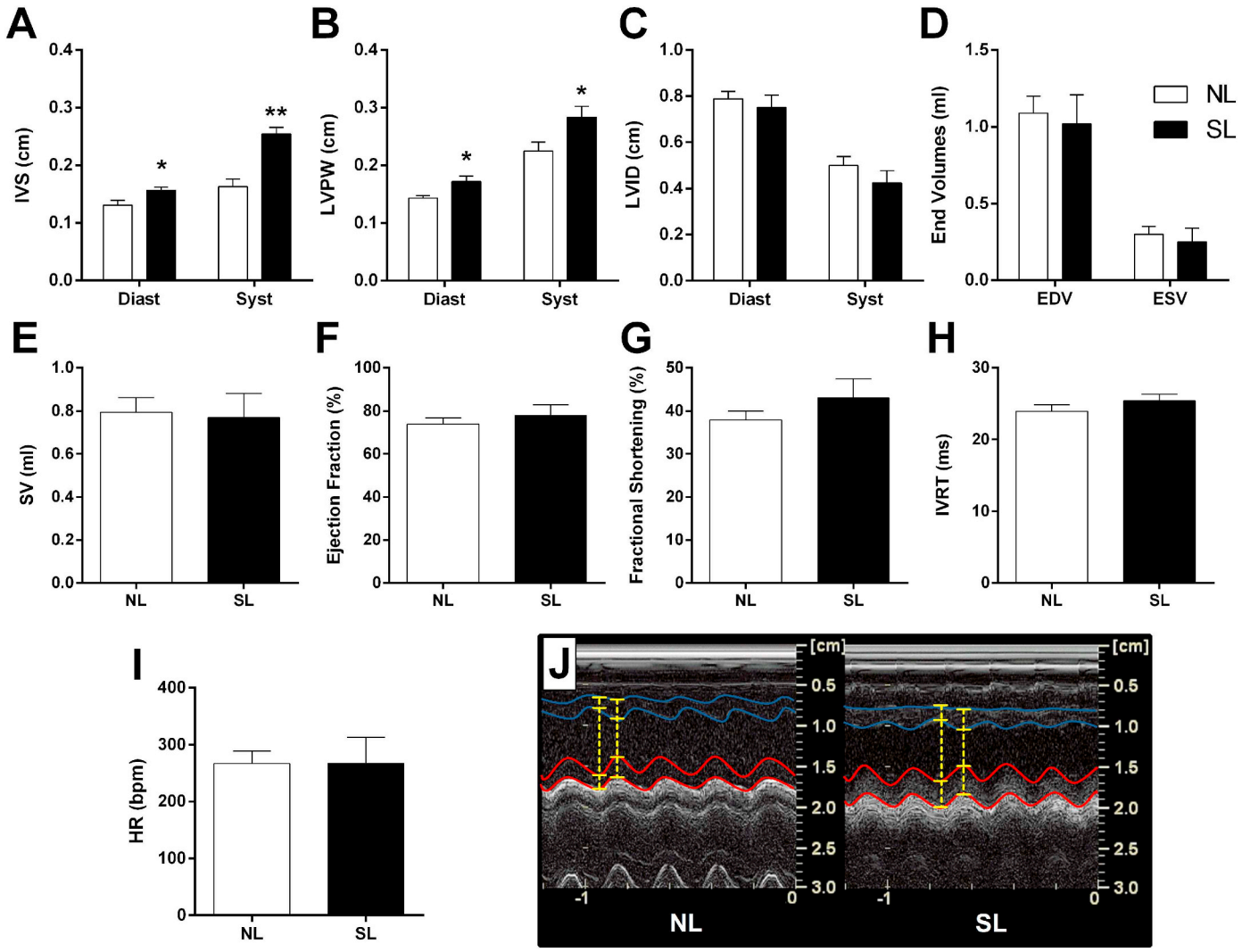

Fig. 2. Effects of postnatal early overfeeding on *in vivo* cardiac morphologic and functionally parameters. Diastolic and systolic thickness of interventricular septum (A), left ventricular posterior wall during systole and diastole (B), estimations of left ventricle internal diameter (C), end diastolic and systolic volumes (D), systolic volume (E), ejection fraction (F), fractional shortening (G), Doppler-based assessment of isovolumetric relaxation time (H), heart rate (I) and representative images of echocardiography of NL and SL animals (J), red lines – limits of LVPW, blue lines – limits of IVS; yellow lines – measurement example. Data are presented as the mean ± SEM. Unpaired Student's *t*-test (n = 6 animals from different litters per group). *p < 0.05 and **p < 0.01 *vs* NL. (For interpretation of the references to colour in this figure legend, the reader is referred to the web version of this article.)

Table 2
Effects of postnatal early overfeeding on blood pressure and heart rate.

Parameter		Group		p value	
		NL	SL		
DBP	mm Hg	87.1 ± 0.67	95.7 ± 2.00	*0.0017*	**
MAP	mm Hg	100.0 ± 0.53	105.5 ± 2.09	*0.0206*	*
SBP	mm Hg	121.3 ± 0.44	135.4 ± 1.30	*< 0.0001*	****
HR	bpm	332 ± 7.03	331 ± 7.21	*0.8914*	*n.s.*

Data are presented as the mean ± SEM. DAP, Diastolic Blood Pressure; MAP, Mean Arterial Pressure; SAP, Systolic Blood Pressure; HR, Heart Rate. Unpaired Student's *t*-test (n = 6 animals from different litters per group).

male Wistar rats. Moreover, we observed endothelial dysfunction, with impaired relaxation and intensified contractile responses. To the best of our knowledge, this study shows for the first time the presence of *ex vivo* impaired cardiovascular function with *in vivo* compensated function in postnatal overfed adult Wistar rats.

Obesity is admittedly a chronic multifactorial disease, which favors the installation of other diseases, or may be an effect of other diseases. Long-term changes in lipid profile, inflammatory state and insulin homeostasis have been correlated with high death rates caused by cardiovascular diseases [36]. Obesity study models commonly use macronutrient-rich diets to induce an increase in body adiposity, especially a high-fat diet [11,22,37]. In our study, we used the PO model, which induces hyperphagia, overweight and high body adiposity, from earliest stages of lactation to adulthood [38,39]. As expected, PO significantly altered body weight of SL animals throughout the experimental period, from the second week of life. The mechanisms that may explain the increase of body mass in the lactation phase are the decrease of competition, and changes in the composition of the dam's milk [38,40]. In this sense, Cancian et al. [40] analyzed the effects of small litter on the dam's breast milk composition, which cause alterations in milk lipid, caloric and protein content. Conversely, our group recently published a study where lactating dams were fed with cafeteria-style diet during the lactation period, promoting increased levels of glucose, triglycerides and cholesterol in the milk, which programmed an obese phenotype in the adult offspring due to hypothalamic alterations and regulating food intake, reinforcing the importance of the breast milk composition in this period of development [22].

Another consequence of PO is the increase in white adipose tissue

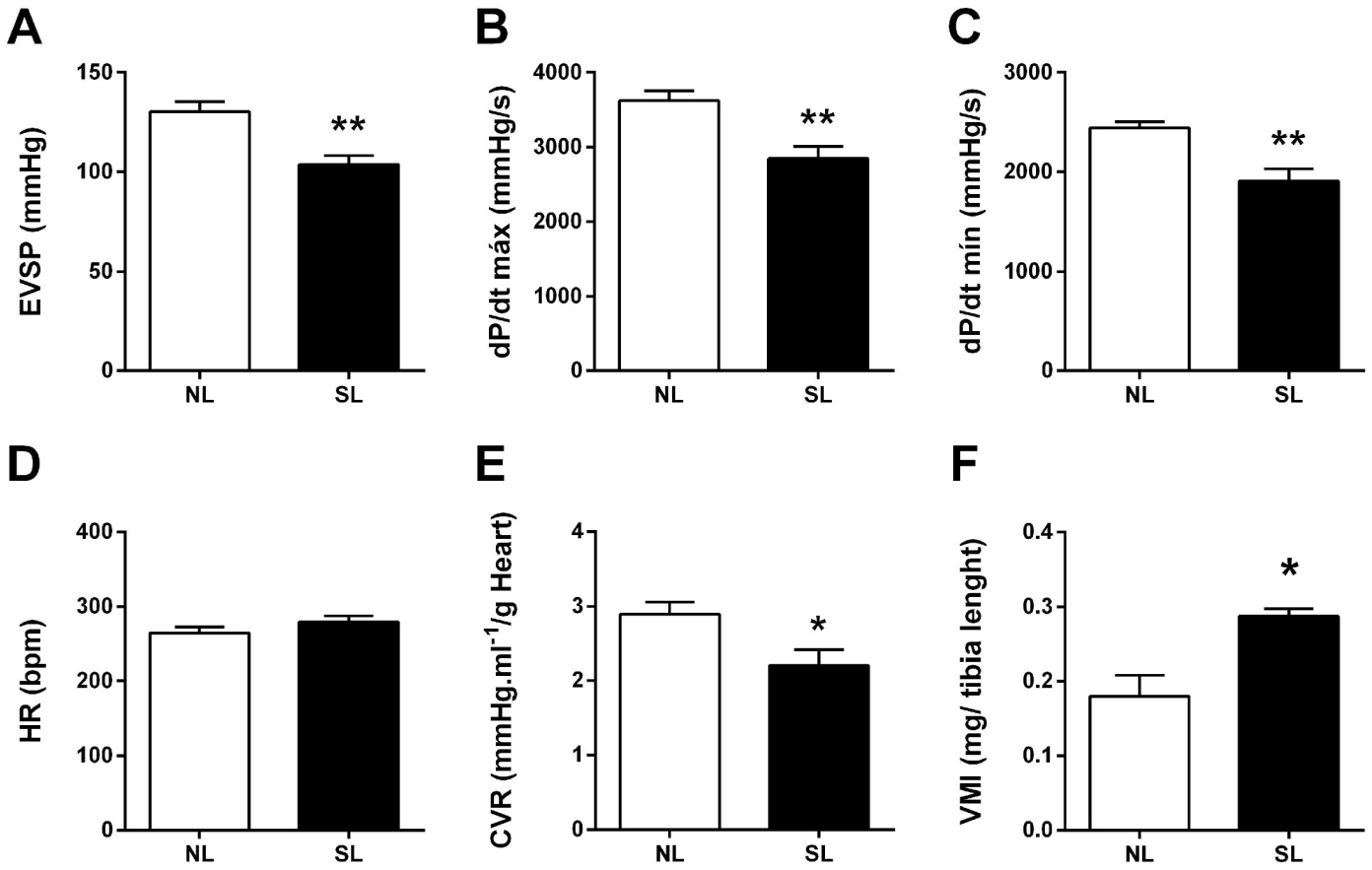

Fig. 3. Effects of postnatal early overfeeding on *ex vivo* cardiac function. End Ventricular Systolic Pressure (A), maximal rate of left ventricular pressure rise (B), maximal rate of left ventricular pressure decline (C), heart rate (D), coronary vascular resistance (E) and ventricular mass index (F). Data are presented as the mean ± SEM. Unpaired Student's *t*-test (n = 5 animals from different litters per group). *p < 0.05 and **p < 0.01 *vs* NL.

stocks due to persistent hyperphagia, which contributes to the imbalance of metabolism, inflammation and raised blood pressure [13,36,41,42]. WAT plays a key role in the endocrine system, secreting both intrinsic hormones, called adipokines, and hormones specific to other metabolic pathways, such as angiotensinogen (AGT) [5,11]. In this work, SL group shows higher adiposity, predominantly mesenteric adipose tissue, and dyslipidemia. Visceral adiposity is frequently correlated with metabolic impairment and dyslipidemia, which promotes a vicious cycle involving lipid accumulation, inflammation, adipocyte dysfunction and AGT overproduction [3,24,32,43].

The role of obesity and AGT overproduction in WAT dysfunction, insulin resistance and genesis of hypertension is not complete understood [6,11,44,45], but is correlated to circulating Angiotensin II levels in obese people [13]. Hypertension causes serious risks to cardiovascular health, promoting changes in cardiac morphology due to mechanic stress or epigenetic alterations, vasomotor responsiveness impairment, or other hemodynamic modifications, which may lead to heart failure [7,18].

SL animals present cardiac hypertrophy without functional impairment *in vivo*. However, *ex vivo* the same hearts showed lower maximum and minimum dP/dt, reduced intraventricular systolic pressure and CVR in the isolated heart preparation. Additionally, SL animals presented raised both systolic and diastolic blood pressure without changes in HR. Other studies evaluated the cardiovascular alterations promoted by PO. Moreira et al. [46] showed that SL animals present early ventricular hypertrophy and reduced myocardial vascularization. Similarly, Ha et al. [41] presented that heart cells of PO young rats were not only more prone to apoptosis, but also more susceptible to replication. Still, Granado et al. [47] reported that hearts of PO animals were more susceptible to ischemia/reperfusion damage, and present contractile deficit due to increased apoptosis. In addition, in our study, adult SL animals presented cardiomyocyte hypertrophy, which is reported in other stages of life [32,34,41]. Our results suggest that SL group is in the compensatory phase of raised arterial pressure, in which extrinsic mechanisms, probably sympathetic nervous system, seem to influence positively the cardiac output.

Other common manifestation of PO on cardiac tissue is the higher collagen deposition, probably due to activation of pro-inflammatory and hypertrophic pathways, such as Reactive Oxygen Species (ROS) mediated pathways [12,48]. In this study, we showed that the hearts of SL rats present higher collagen deposition in both interstitial and perivascular areas, this data is in agreement with the decreased contractile function observed in the isolated hearts. Indeed, increased SOD-1 expression, with no differences in CAT expression or Akt/eNOS pathway, suggests impaired protection against oxidative stress.

Despite morphological and oxidative stress alterations, the expression of the main receptors of the RAS signaling was not modified in the heart of SL animals. The protein quantification reported in our study is in agreement with the quantifications of gene transcription reported by Granado et al. [47], in which there was no difference in the gene expression for AT1 and AT2 receptors. Here, the expression of MASR was evaluated in PO animals at adulthood, revealing for the first time, that not only the absence of changes in AT2R expression occurs. In this sense, epigenetic alterations must be the major cause of cardiac alterations due to PO. Although no changes in RAS in the adult heart of PO animals, early alterations in local RAS of young PO rats promotes Renin and AT2R upregulation at 28th day of life, that could attempt to protect the heart against PO negative effects [41]. RAB1 is closely related to the transport of receptors involved in the regulation of cardiac function and morphology and even in the response to activation of

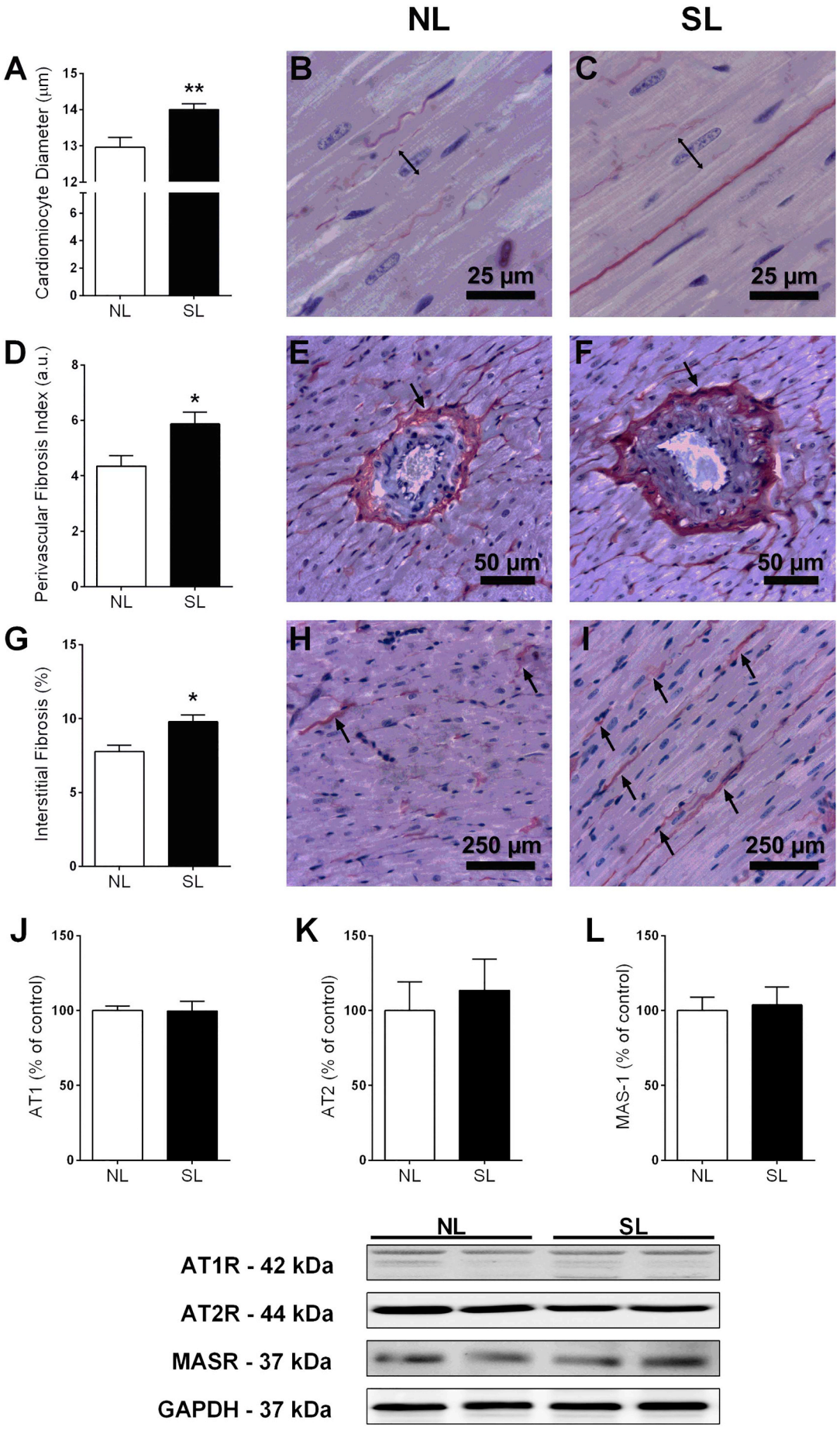

(caption on next page)

Fig. 4. Effects of postnatal early overfeeding on cardiac morphology parameters and angiotensin receptors expression in the heart. Cardiomyocyte diameter (A) and representative photomicrographs (×1000 magnification, scale bars = 25 μm) showing cardiomyocytes transversal sections from NL (B) and SL (C) animals stained with picrosirius red and hematoxylin. Perivascular fibrosis index (D) and representative photomicrographs (×400 magnification, scale bars = 50 μm) showing ventricular vessels transversal sections from NL (E) and SL (F) animals stained with picrosirius red and hematoxylin. Interstitial fibrosis (G) and representative photomicrographs (×100 magnification, scale bars = 250 μm) showing longitudinal sections of left ventricles from NL (H) and SL (I) animals stained with picrosirius red and hematoxylin. Data are presented as the mean ± SEM. Unpaired Student's *t*-test (n = 5 animals from different litters per group). *p < 0.05 and **p < 0.01 *vs* NL. Black arrows indicate picrosirius stained collagen. Western blot analysis of AT1R (J), AT2R (K) and MASR (L). Representative immunoblots are show below the graphs. Data are presented as the mean ± SEM of each group, normalized to GAPDH density. Unpaired Student's *t*-test. (For interpretation of the references to colour in this figure legend, the reader is referred to the web version of this article.)

these receptors, such as AT1R and adrenergic receptors [49–51]. Interestingly, despite the increase in RAB-1b expression and cardiac remodeling, there was no difference in the expression of AT1R receptors in the left ventricle of the SL animals, which may indicate the activation of other receptors that can mediate the remodeling [51].

In parallel to morphological changes, metabolic impairment due to

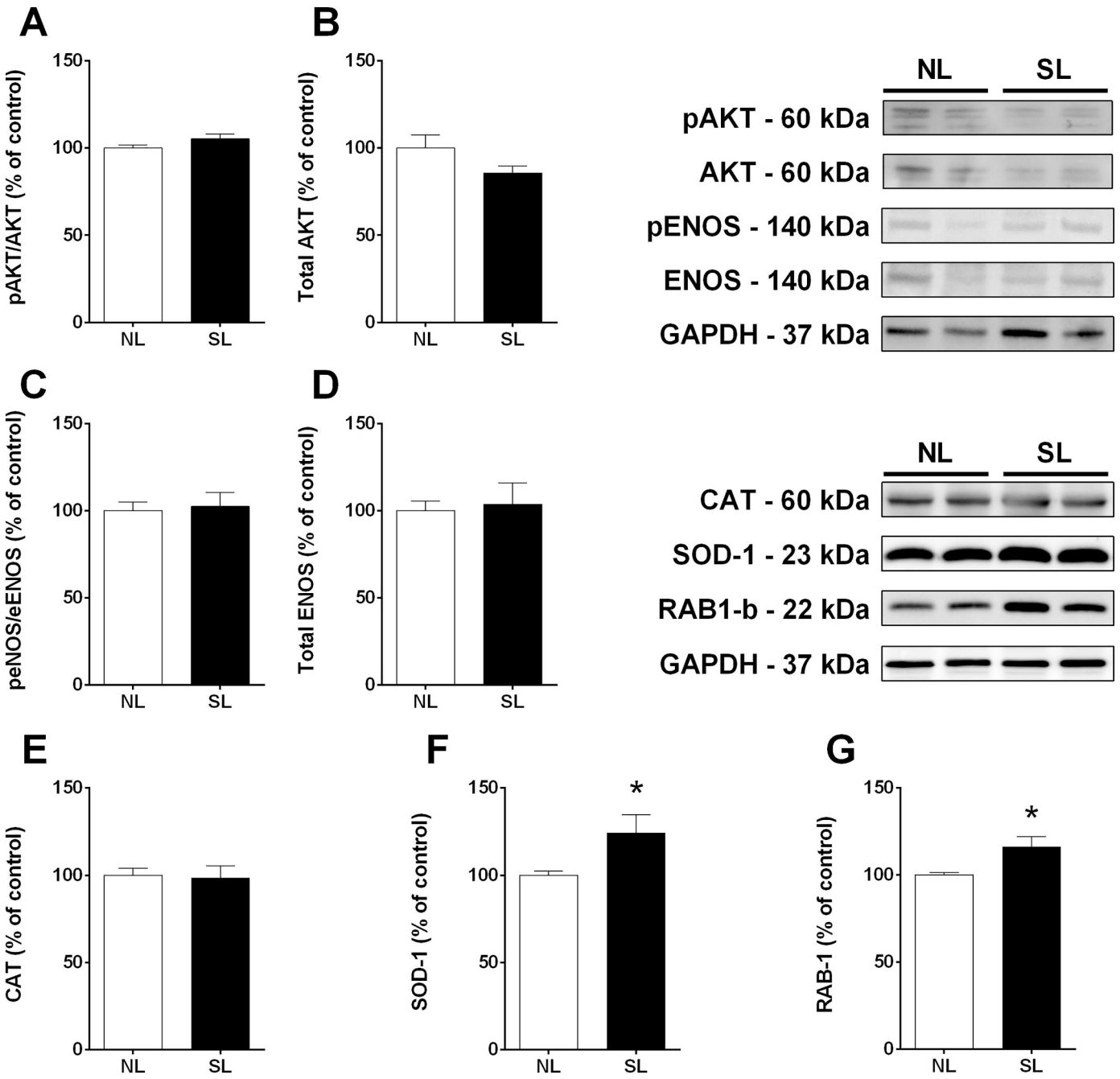

Fig. 5. Effects of postnatal early overfeeding on Akt, eNOS, CAT, SOD-1 and RAB1-b expression in the heart. Western blot analysis of pAkt/Akt (A), total Akt (B), peNOS/eNOS (C), total eNOS (D), CAT (E), SOD-1 (F) and RAB-1b (G). Representative immunoblots are show on the up-right corner. Data are presented as the mean ± SEM of each group, normalized to GAPDH density. Unpaired Student's *t*-test. *p < 0.05 *vs* NL.

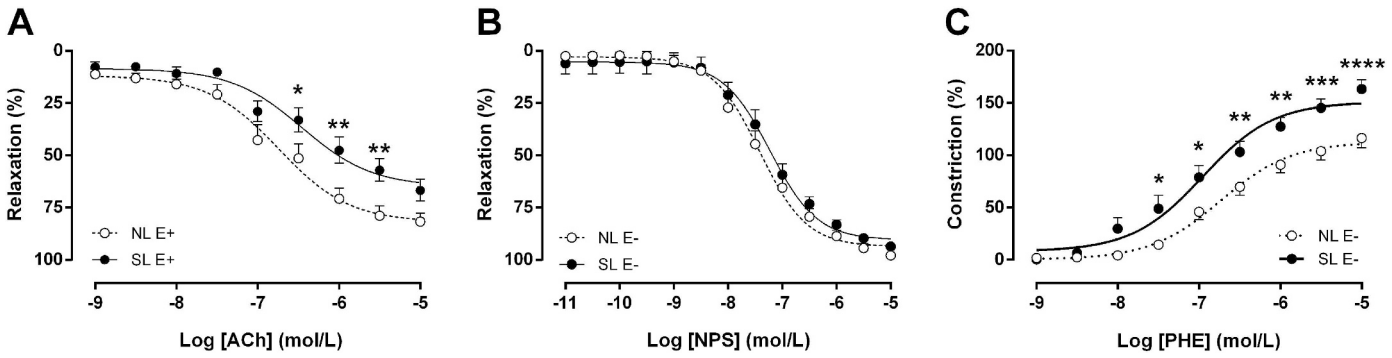

Fig. 6. Effects of postnatal early overfeeding on aorta vasocontractility. Acetylcholine induced relaxation of e+ aorta rings (A), sodium nitroprusside induced relaxation of e− aorta rings (b) and phenylephrine induced constriction of e− aorta rings (C). Data are presented as the mean ± SEM. Two-way ANOVA and Sidak's *post-hoc* test (n = 5 animals from different litters per group). *p < 0.05, **p < 0.01, ***p < 0.001 and ****p < 0.0001 *vs* NL.

insulin resistance occurs in cardiac tissue, which may contribute to the contractile alterations observed in our study and in other studies [16,52]. Insulin resistance also is a detrimental factor in vascular function, which decreases the endothelial-dependent relaxant response, and contributes to increased ROS formation and raised blood pressure [15,21]. In this sense, Novo et al. [14] correlated several metabolic and cardiovascular parameters, finding positive values for the correlation between insulin resistance and arterial stiffness, and between insulin resistance and left ventricular hypertrophy. Thus, the mechanisms by which cardiac remodeling occurs appear to be related to pressure overload due to endothelial dysfunction, and changes in the phenotype due to metabolic malprogramming.

Certainly, one of the most influential parameters in systolic blood pressure is the post-load, characterized mainly by systemic vascular resistance (SVR). In turn, SVR is could be caused by deficiency in vasomotor responses, especially to relaxation stimuli. Here, aortic rings from SL animals had a lower acetylcholine-mediated vasorelaxation, but without significant changes in the response to sodium nitroprusside (NPS). Despite these data suggest the presence of endothelial dysfunction, the coronary vascular resistance was lower in SL than in NL group. The difference in the response between aorta and coronary bed can be due to the functional difference among the vessels, since aorta is known as conductance artery while, in isolated hearts, it was evaluated a resistance vascular bed. However, this parameter should be addressed properly by future studies. Similar studies showed the vascular dysfunction in PO animals. Sánchez-García et al. [19] showed that aorta of PO animals present more collagen and elastic fibers content. The vasodilatory responses to NPS are a result of the direct action of nitric oxide (NO) on the contractile machinery, unlike the action of ACh that acts in the stimulation of the enzyme eNOS (endothelial nitric oxide synthase) from the influx of Ca^{2+} ions by the ionotropic receptor of Ach [53]. Thus, eNOS impairment in the vascular endothelium of the SL group probably mediates the lower relaxation results observed *ex vivo*, together with a greater responsiveness to the adrenergic contractile action also observed in *ex vivo* tests, compared to the respective controls. As one, insulin resistance and ROS generation appear to promote vascular dysfunction by reducing NO bioavailability in this animal model. Our results consolidate the knowledge that the PO during lactation is critical for cardiometabolic programming. This phenomenon is mainly due to the vulnerability of the heart to environmental changes during early life, leading to oxidative stress and cardiac remodeling.

5. Conclusion

Taken together, our data suggest that the SL animals have compensated cardiovascular function and oxidative stress despite the of cardiac remodeling, both results might be origin in increased body adiposity, due to hyperphagic behavior and epigenetic alterations onset during lactation. These data indicate that overnutrition during perinatal life compromised cardiac function in adulthood, which turn into an alert to take more care in early life, which ensure better health in the later stages of life.

Declaration of interest

The authors declare that there are no conflicts of interest.

Funding

This work was funded by the Brazilian Foundations: Conselho Nacional de Desenvolvimento Científico e Tecnológico (CNPq), Coordenação de Aperfeiçoamento de Pessoal de Nível Superior (CAPES), and Fundação de Amparo à Pesquisa do Estado de Goiás (FAPEG).

Author contributions

Marcos D. Ferreira Junior: Conceptualization, Methodology, Investigation, Writing – Original draft, Writing – Review and Editing. *Keilah V.N. Cavalcante*: Investigation, Writing – Review and Editing. *Lucas A. Ferreira*: Investigation, Writing – Review and Editing. *Paulo R. Lopes*: Methodology. *Carolina N.R. Pontes*: Investigation, Writing – Review and Editing. *Amanda S.M. Bessa*: Investigation, Writing – Review and Editing. *Ângela R. Neves*: Methodology, Investigation. *Flávio A. Francisco*: Investigation, Writing – Review and Editing. *Gustavo R. Pedrino*: Resources. *Carlos H.X. Custódio*: Resources. *Paulo C.F. Mathias*: Methodology, Resources, Writing – Review and Editing. *Carlos H. Castro*: Conceptualization, Methodology, Resources, Writing – Review and Editing. *Rodrigo M. Gomes*: Conceptualization, Methodology, Resources, Writing – Original draft, Writing – Review and Editing.

References

[1] N. Chevalier, P. Fénichel, Obésité, diabète de type 2 et perturbateurs endocriniens, Press. Medicale. 45 (2016) 88–97, https://doi.org/10.1016/j.lpm.2015.08.008.
[2] T. Kelly, W. Yang, C.-S. Chen, K. Reynolds, J. He, Global burden of obesity in 2005 and projections to 2030, Int. J. Obes. 32 (2008) 1431–1437, https://doi.org/10.1038/ijo.2008.102.
[3] M. Bastien, P. Poirier, I. Lemieux, J.P. Després, Overview of epidemiology and contribution of obesity to cardiovascular disease, Prog. Cardiovasc. Dis. 56 (2014) 369–381, https://doi.org/10.1016/j.pcad.2013.10.016.
[4] H. Azzam, S. Malnick, Non-alcoholic fatty liver disease - the heart of the matter, World J. Hepatol. 7 (2015) 1369–1376, https://doi.org/10.4254/wjh.v7.i10.1369.
[5] M. Guerre-Millo, Adipose tissue and adipokines: for better or worse, Diabetes Metab. 30 (2004) 13–19, https://doi.org/10.1016/S1262-3636(07)70084-8.
[6] F. Yiannikouris, M. Gupte, K. Putnam, S. Thatcher, R. Charnigo, D.L. Rateri, A. Daugherty, L.A. Cassis, Adipocyte deficiency of angiotensinogen prevents obesity-induced hypertension in male mice, Hypertension 60 (2012) 1524–1530, https://doi.org/10.1161/HYPERTENSIONAHA.112.192690.
[7] M.E. Frigolet, N. Torres, A.R. Tovar, The renin-angiotensin system in adipose tissue

and its metabolic consequences during obesity, J. Nutr. Biochem. 24 (2013) 2003–2015, https://doi.org/10.1016/j.jnutbio.2013.07.002.
[8] A.R. Johnson, J.J. Milner, L. Makowski, The inflammation highway: metabolism accelerates inflammatory traffic in obesity, Immunol. Rev. 249 (2012) 218–238, https://doi.org/10.1111/j.1600-065X.2012.01151.x.
[9] H. Cao, Adipocytokines in obesity and metabolic disease, J. Endocrinol. 220 (2014) T47–T59, https://doi.org/10.1530/JOE-13-0339.
[10] N.K. Littlejohn, J.L. Grobe, Opposing tissue-specific roles of angiotensin in the pathogenesis of obesity, and implications for obesity-related hypertension, Am. J. Phys. Regul. Integr. Comp. Phys. 309 (2015) R1463–R1473, https://doi.org/10.1152/ajpregu.00224.2015.
[11] N.S. Kalupahana, F. Massiera, A. Quignard-Boulange, G. Ailhaud, B.H. Voy, D.H. Wasserman, N. Moustaid-Moussa, Overproduction of angiotensinogen from adipose tissue induces adipose inflammation, glucose intolerance, and insulin resistance, Obesity 20 (2012) 48–56, https://doi.org/10.1038/oby.2011.299.
[12] P.R. De Batista, R. Palacios, A. Martín, R. Hernanz, C.T. Médici, M.A.S.C. Silva, E.M. Rossi, A. Aguado, D.V. Vassallo, M. Salaices, M.J. Alonso, Toll-like receptor 4 upregulation by angiotensin II contributes to hypertension and vascular dysfunction through reactive oxygen species production, PLoS One 9 (2014) e104020, , https://doi.org/10.1371/journal.pone.0104020.
[13] A. Saiki, M. Ohira, K. Endo, N. Koide, T. Oyama, T. Murano, H. Watanabe, Y. Miyashita, K. Shirai, Circulating angiotensin II is associated with body fat accumulation and insulin resistance in obese subjects with type 2 diabetes mellitus, Metabolism 58 (2009) 708–713, https://doi.org/10.1016/j.metabol.2009.01.013.
[14] G. Novo, G. Manno, R. Russo, D. Buccheri, S. Dell'Oglio, P. Morreale, G. Evola, G. Vitale, S. Novo, Impact of insulin resistance on cardiac and vascular function, Int. J. Cardiol. 221 (2016) 1095–1099, https://doi.org/10.1016/j.ijcard.2016.07.087.
[15] G. Lastra, C. Manrique, Perivascular adipose tissue, inflammation and insulin resistance: link to vascular dysfunction and cardiovascular disease, Horm. Mol. Biol. Clin. Invest. 22 (2015) 1–8, https://doi.org/10.1515/hmbci-2015-0010.
[16] M.R. Martins, A.K. Gonzalez Vieira, É.P. Garcia de Souza, A.S. Moura, Early overnutrition impairs insulin signaling in the heart of adult Swiss mice, J. Endocrinol. 198 (2008) 591–598, https://doi.org/10.1677/JOE-08-0057.
[17] L. Mazzolai, T. Pedrazzini, F. Nicoud, G. Gabbiani, H.R. Brunner, J. Nussberger, Increased cardiac angiotensin II levels induce right and left ventricular hypertrophy in normotensive mice, Hypertension 35 (2000) 985–991, https://doi.org/10.1161/01.HYP.35.4.985.
[18] W. Nadruz, A.M. Shah, S.D. Solomon, Diastolic dysfunction and hypertension, Med. Clin. North Am. 101 (2017) 7–17, https://doi.org/10.1016/j.mcna.2016.08.013.
[19] G. Sánchez-García, L. Del Bosque-Plata, E. Hong, Postnatal overnutrition affects metabolic and vascular function reflected by physiological and histological changes in the aorta of adult Wistar rats, Clin. Exp. Hypertens. 00 (2017) 1–9, https://doi.org/10.1080/10641963.2017.1392557.
[20] A. Habbout, S. Delemasure, F. Goirand, J.C. Guilland, F. Chabod, M. Sediki, L. Rochette, C. Vergely, Postnatal overfeeding in rats leads to moderate overweight and to cardiometabolic and oxidative alterations in adulthood, Biochimie 94 (2012) 117–124, https://doi.org/10.1016/j.biochi.2011.09.023.
[21] R. Li, H. Zhang, W. Wang, X. Wang, Y. Huang, C. Huang, F. Gao, Vascular insulin resistance in prehypertensive rats: role of PI3-kinase/Akt/eNOS signaling, Eur. J. Pharmacol. 628 (2010) 140–147, https://doi.org/10.1016/j.ejphar.2009.11.038.
[22] R.M. Gomes, F.G. Bueno, C.R. Schamber, J.C.P. de Mello, J.C. de Oliveira, F.A. Francisco, V.M. Moreira, M.D.F. Junior, G.R. Pedrino, P.C. de Freitas Mathias, R.A. Miranda, S.M.F. de Moraes, M.R.M. Natali, Maternal diet-induced obesity during suckling period programs offspring obese phenotype and hypothalamic leptin/insulin resistance, J. Nutr. Biochem. 61 (2018) 24–32, https://doi.org/10.1016/j.jnutbio.2018.07.006.
[23] E.P.S. Conceição, J.G. Franco, E. Oliveira, A.C. Resende, T.A.S. Amaral, N. Peixoto-Silva, M.C.F. Passos, E.G. Moura, P.C. Lisboa, Oxidative stress programming in a rat model of postnatal early overnutrition - role of insulin resistance, J. Nutr. Biochem. 24 (2013) 81–87, https://doi.org/10.1016/j.jnutbio.2012.02.010.
[24] B.D. Kayser, M.I. Goran, S.G. Bouret, Perinatal overnutrition exacerbates adipose tissue inflammation caused by high-fat feeding in C57BL/6J mice, PLoS One 10 (2015) 1–15, https://doi.org/10.1371/journal.pone.0121954.
[25] N. Zeeni, C. Dagher-Hamalian, H. Dimassi, W.H. Faour, Cafeteria diet-fed mice is a pertinent model of obesity-induced organ damage: a potential role of inflammation, Inflamm. Res. 64 (2015) 501–512, https://doi.org/10.1007/s00011-015-0831-z.
[26] F.C. Cassidy, M. Charalambous, Genomic imprinting, growth and maternal–fetal interactions, J. Exp. Biol. 221 (2018) jeb164517, , https://doi.org/10.1242/jeb.164517.
[27] C. Junien, P. Panchenko, S. Fneich, L. Pirola, S. Chriett, V. Amarger, B. Kaeffer, P. Parnet, J. Torrisani, F. Bolanõs Jimenez, H. Jammes, A. Gabory, Épigénétique et réponses transgénérationnelles aux impacts de l'environnement: Des faits aux lacunes, Medecine/Sciences 32 (2016) 35–44, https://doi.org/10.1051/medsci/20163201007.
[28] M.C. Hallam, R.A. Reimer, Impact of diet composition in adult offspring is dependent on maternal diet during pregnancy and lactation in rats, Nutrients 8 (2016) 46, https://doi.org/10.3390/nu8010046.
[29] M.H. Vickers, Z.E. Clayton, C. Yap, D.M. Sloboda, Maternal fructose intake during pregnancy and lactation alters placental growth and leads to sex-specific changes in fetal and neonatal endocrine function, Endocrinology 152 (2011) 1378–1387, https://doi.org/10.1210/en.2010-1093.
[30] F.A. Francisco, L.F. Barella, S. da S. Silveira, L.P.J. Saavedra, K.V. Prates, V.S. Alves, C.C. da S. Franco, R.A. Miranda, T.A. Ribeiro, L.P. Tófolo, A. Malta, E. Vieira, K. Palma-Rigo, A. Pavanello, I.P. Martins, V.M. Moreira, J.C. de Oliveira, P.C. de F. Mathias, R.M. Gomes, Methylglyoxal treatment in lactating mothers leads to type 2 diabetes phenotype in male rat offspring at adulthood, Eur. J. Nutr. 57 (2018) 477–486, https://doi.org/10.1007/s00394-016-1330-x.
[31] T.A. Ribeiro, L.P. Tófolo, I.P. Martins, A. Pavanello, J.C. de Oliveira, K.V. Prates, R.A. Miranda, C.C. da Silva Franco, R.M. Gomes, F.A. Francisco, V.S. Alves, D.L. de Almeida, V.M. Moreira, K. Palma-Rigo, E. Vieira, G.S. Fabricio, M.R. da Silva Rodrigues, W. Rinaldi, A. Malta, P.C. de Freitas Mathias, Maternal low intensity physical exercise prevents obesity in offspring rats exposed to early overnutrition, Sci. Rep. 7 (2017) 7634, , https://doi.org/10.1038/s41598-017-07395-2.
[32] A. Habbout, N. Li, L. Rochette, C. Vergely, Postnatal overfeeding in rodents by litter size reduction induces major short- and long-term pathophysiological consequences, J. Nutr. 143 (2013) 553–562, https://doi.org/10.3945/jn.112.172825.
[33] F. Bei, J. Jia, Y.-Q. Jia, J.-H. Sun, F. Liang, Z.-Y. Yu, W. Cai, Long-term effect of early postnatal overnutrition on insulin resistance and serum fatty acid profiles in male rats, Lipids Health Dis. 14 (2015) 96, https://doi.org/10.1186/s12944-015-0094-2.
[34] A. Habbout, C. Guenancia, J. Lorin, E. Rigal, C. Fassot, L. Rochette, C. Vergely, Postnatal overfeeding causes early shifts in gene expression in the heart and long-term alterations in cardiometabolic and oxidative parameters, PLoS One 8 (2013), https://doi.org/10.1371/journal.pone.0056981.
[35] W.T. Friedewald, R.I. Levy, D.S. Fredrickson, Estimation of the concentration of low-density lipoprotein cholesterol in plasma, without use of the preparative ultracentrifuge, Clin. Chem. 18 (1972) 499–502 http://www.ncbi.nlm.nih.gov/pubmed/4337382.
[36] J. Upadhyay, O. Farr, N. Perakakis, W. Ghaly, C. Mantzoros, Obesity as a disease, Med. Clin. North Am. 102 (2018) 13–33, https://doi.org/10.1016/j.mcna.2017.08.004.
[37] S.M. Alwahsh, B.J. Dwyer, S. Forbes, D.H. van Thiel, P.J. Starkey Lewis, G. Ramadori, Insulin production and resistance in different models of diet-induced obesity and metabolic syndrome, Int. J. Mol. Sci. 18 (2017), https://doi.org/10.3390/ijms18020285.
[38] Š. Mozeš, Z. Šefčíková, L. Raček, Long-term effect of altered nutrition induced by litter size manipulation and cross-fostering in suckling male rats on development of obesity risk and health complications, Eur. J. Nutr. 53 (2014) 1273–1280, https://doi.org/10.1007/s00394-013-0630-7.
[39] P. Argente-Arizón, P. Ros, F. Díaz, E. Fuente-Martin, D. Castro-González, M.Á. Sánchez-Garrido, V. Barrios, M. Tena-Sempere, J. Argente, J.A. Chowen, Age and sex dependent effects of early overnutrition on metabolic parameters and the role of neonatal androgens, Biol. Sex Differ. 7 (2016) 26, , https://doi.org/10.1186/s13293-016-0079-5.
[40] C.R.C. Cancian, N.C. Leite, E.G. Montes, S.V. Fisher, L. Waselcoski, E.C.L. Stal, R.Z. Christoforo, S. Grassiolli, Histological and metabolic state of dams suckling small litter or MSG-treated pups, Sci. World J. 2016 (2016) 1–12, https://doi.org/10.1155/2016/1678541.
[41] K.S. Ha, K.H. Yoo, H.E. Yim, G.Y. Jang, I.S. Bae, Y.S. Hong, J.W. Lee, Cellular and RAS changes in the hearts of young obese rats, Pediatr. Cardiol. 32 (2011) 659–666, https://doi.org/10.1007/s00246-011-9952-5.
[42] M. Pahlavani, N.S. Kalupahana, L. Ramalingam, N. Moustaid-Moussa, M. Pahlavani, N.S. Kalupahana, L. Ramalingam, N. Moustaid-Moussa, Regulation and functions of the renin-angiotensin system in white and brown adipose tissue, Compr. Physiol. 7 (2017) 1137–1150, https://doi.org/10.1002/CPHY.C160031.
[43] H.F. Lopes, M. Lúcia, C. Giannella, F.M.C. Colombo, B.M. Egan, Visceral adiposity syndrome, Diabetol. Metab. Syndr. 8 (1) (2016), https://doi.org/10.1186/s13098-016-0156-2.
[44] F. Massiera, J. Seydoux, A. Geloen, A. Quignard-Boulange, S. Turban, P. Saint-Marc, A. Fukamizu, R. Negrel, G. Ailhaud, M. Teboul, Angiotensinogen-deficient mice exhibit impairment of diet-induced weight gain with alteration in adipose tissue development and increased locomotor activity, Endocrinology 142 (2001) 5220–5225, https://doi.org/10.1210/endo.142.12.8556.
[45] T. de A. Pinheiro, A.S. Barcala-Jorge, J.M.O. Andrade, T. de A. Pinheiro, E.C.N. Ferreira, T.S. Crespo, G.C. Batista-Jorge, C.A. Vieira, D. de F. Lelis, A.F. Paraíso, U.B. Pinheiro, M. Bertagnolli, C.J.B. Albuquerque, A.L.S. Guimarães, A.M.B. de Paula, A.P. Caldeira, S.H.S. Santos, Obesity and malnutrition similarly alters the renin–angiotensin system and inflammation in mice and human adipose, J. Nutr. Biochem. 48 (2017) 74–82, https://doi.org/10.1016/j.jnutbio.2017.06.008.
[46] A.S.B. Moreira, M. Teixeira Teixeira, F. da Silveira Osso, R.O. Pereira, G. de Oliveira Silva-Junior, E.P. Garcia de Souza, C.A. Mandarim de Lacerda, A.S. Moura, Left ventricular hypertrophy induced by overnutrition early in life, Nutr. Metab. Cardiovasc. Dis. 19 (2009) 805–810, https://doi.org/10.1016/j.numecd.2009.01.008.
[47] M. Granado, N. Fernández, L. Monge, G. Carreño-Tarragona, J.C. Figueras, S. Amor, Á.L. García-Villalón, Long-term effects of early overnutrition in the heart of male adult rats: role of the renin-angiotensin system, PLoS One 8 (2013) 1–11, https://doi.org/10.1371/journal.pone.0065172.
[48] R.A.S. Santos, C.H. Castro, E. Gava, S.V.B. Pinheiro, A.P. Almeida, R.D. De Paula, J.S. Cruz, A.S. Ramos, K.T. Rosa, M.C. Irigoyen, M. Bader, N. Alenina, G.T. Kitten, A.J. Ferreira, Impairment of in vitro and in vivo heart function in angiotensin-(1–7) receptor mas knockout mice, Hypertension 47 (2006) 996–1002, https://doi.org/10.1161/01.HYP.0000215289.51180.5c.
[49] C.M. Filipeanu, F. Zhou, G. Wu, Analysis of Rab1 function in cardiomyocyte growth, Methods Enzymol. 438 (2008) 217–226, https://doi.org/10.1016/S0076-6879(07)38015-4.
[50] L. Wei, M. Yuan, R. Zhou, Q. Bai, W. Zhang, M. Zhang, Y. Huang, L. Shi, MicroRNA-101 inhibits rat cardiac hypertrophy by targeting Rab1a, J. Cardiovasc. Pharmacol. 65 (2015) 357–363, https://doi.org/10.1097/FJC.0000000000000203.
[51] G. Wu, G. Zhao, Y. He, Distinct pathways for the trafficking of angiotensin II and adrenergic receptors from the endoplasmic reticulum to the cell surface: Rab1-independent transport of a G protein-coupled receptor, J. Biol. Chem. 278 (2003)

47062–47069, https://doi.org/10.1074/jbc.M305707200.
[52] A.F. Bernardo, E. Cortez, F.A. Neves, A.K.G. Vieira, V. de M. Soares, A.C.d.S. Rodrigues-Cunha, D.C. Andrade, A.A. Thole, D. Gabriel-Costa, P.C. Brum, A.S. Moura, É.P. Garcia-Souza, Overnutrition during lactation leads to impairment in insulin signaling, up-regulation of GLUT1 and increased mitochondrial carbohydrate oxidation in heart of weaned mice, J. Nutr. Biochem. 29 (2016) 124–132, https://doi.org/10.1016/j.jnutbio.2015.09.021.
[53] P. Kandavelu, N. Yuldasheva, P. Sukumar, J. Smith, D.J. Beech, V.K. Gatenby, M. Gage, M.T. Kearney, A. Skromna, H. Viswambharan, S. Galloway, H. Imrie, R.M. Cubbon, A.M. Shah, K.M. Channon, S.B. Wheatcroft, C.X. Santos, Nox2 NADPH oxidase has a critical role in insulin resistance-related endothelial cell dysfunction, Diabetes 62 (2013) 2130–2134, https://doi.org/10.2337/db12-1294.